

## Real-Time Surveillance Performance under Different Sensing Models in Duty-Cycled Sensor Networks

Yanjun Li

School of Computer Science and Technology, Zhejiang University of Technology,  
288 Liuhe Road, Hangzhou 310023, China  
Tel.: +86-571-85290527, Fax: +86-571-85290668  
E-mail: [yjli@zjut.edu.cn](mailto:yjli@zjut.edu.cn)

Received: 28 May 2013 / Accepted: 25 August 2013 / Published: 30 September 2013

---

**Abstract:** In this paper, we derive closed-form expressions to describe the relationship between the surveillance quality and system parameters under different real-time requirements and arbitrary sensing models, where the surveillance quality is represented by real-time intrusion detection probability and the system parameters are represented by duty cycle factors and node density. Various sensing models are adopted in the numerical simulations, including Boolean disk model, exponential model, power-law model, staircase model and anisotropic model, to validate the analytical closed-form results. It is shown that under all these sensing models adopted, the numerical results always closely matches the analytical ones, which soundly verifies the correctness of our derivation. *Copyright © 2013 IFSA.*

**Keywords:** Real-Time, Sensing Model, Duty-Cycle, Sensor Networks.

---

### 1. Introduction

For many long-term unattended applications such as environmental monitoring, infrastructure protection and military surveillance, wireless sensor networks (WSNs) have become one of the most effective solutions, due to their pervasive sensing, computing and self-organizing capabilities. One common goal for these surveillance applications is the real-time detection of abnormal states or intrusion targets with minimal energy consumption. However, detection timeliness and energy efficiency are to some extent two contradictive objectives. For example, full duty-cycled sensing guarantees instant response to events, but it is not energy-efficient. On the contrary, low duty cycle can extend the network lifetime but makes the sensing ability intermitted, which will adversely affect the surveillance quality, e.g., increasing the detection delay. Sometimes

surveillance quality can be sacrificed within users' tolerable limits for prolonged lifetime. Therefore, it is required to understand the relationship that describes the tradeoffs between surveillance quality and system parameters, e.g., the relationship between the detection probability, the detection delay, the duty cycle factor and the node density etc. With this knowledge, an appropriate set of parameters can be selected to configure the network for achieving required surveillance performance.

In this paper, we aim to establish the relationship between the surveillance quality and system parameters under different real-time requirements and arbitrary sensing models. We make two major contributions in this paper. First, closed-form expressions are obtained to specify the above-mentioned relationship. The advantage is that we can now answer a variety of questions without simulations or experiments, e.g., under an arbitrary

sensing model and a specific detection delay bound, how much should we set the sensor's duty cycle factor or the node density to achieve a required detection probability? Second, different sensing models are adopted in the numerical simulations to validate the analytical closed-form results. It has been shown that under all these sensing models adopted, the numerical results always closely matches the analytical ones.

The remaining of the paper is organized as follows. Section 2 discusses related work. Section 3 derives the closed-form expressions for detection probability. Numerical simulations are conducted in Section 4. Finally Section 5 concludes the paper.

## 2. Related Work

Research on energy efficiency and real-time performance has been highly investigated by the sensor network community in recent years. We here briefly review only a handful of the most related work to this study. The work in [1] studies the quality and energy tradeoffs for mobile object tracking in WSNs. Various activation strategies are discussed. The work in [2-4] presents the real-time design and analysis of VigilNet, a large-scale sensor network system which detects and classifies objects in a timely and energy efficient manner. It provides a design framework to guarantee the requested end-to-end deadline. The power management system composes of both sentry and non-sentry nodes where non-sentry nodes are sleep unless sentry nodes activate them. The work in [5] analyzes the accuracy of tracking vs. response latency to the tracking queries, as well as the effect of duty-cycle parameters on the quality metrics. The sensors assumed in previous work [1, 3-6] are binary detectors, i.e., Boolean disk sensing model, except in [2], anisotropic sensing model is also considered. However, none of the above work incorporates the fading effect of sensing ability into consideration. The contribution of our work compared to previous derivation is in obtaining a general result for real-time surveillance performance in duty-cycled WSNs for arbitrary sensing models, including Boolean disk model, exponential model, power-law model, staircase model and anisotropic model. We believe our work a necessary complement towards thorough understanding of the detection performance.

## 3. Detection Performance Analysis

In this section, we analyze the probability distribution of the detection delay  $t$  for any given delay bound  $\tau$ .

### 3.1. Notations and Assumptions

Some notations and assumptions for analysis are presented here. First of all, we assume the nodes are

independently and identically distributed conforming to homogeneous Poisson point process (P.P.P.) with intensity  $\lambda_A$ , where  $\lambda_A$  is defined as the node density  $d$  multiplying the area in which nodes are deployed, denoted by  $A$ . In our analysis, we first assume the probability that an event at point  $P$  be sensed by sensor  $S_i$  to be  $p(x)$ , where  $p(x)$  can be an arbitrary function depending on the distance  $x$ , which means  $p$  can be viewed as a function  $p: \mathbb{R} \rightarrow [0, 1]$ . In fact, besides the distance between the sensor and the actual event, the sensing quality also depends on other factors, for example, the directionality and the environmental noise. However, to make the problem less complicated, we mainly focus on the distance aspect and assume omnidirectional sensing and no random noise, just as most of the sensing models in the literature do. However, in the simulation part, we also take anisotropic sensing model into consideration. Based on the above assumptions, the average number of nodes within the coverage area of a sensor can be calculated as:

$$\lambda_c = d \cdot \int_{x \in \mathbb{R}} 2\pi x p(x) dx, \quad (1)$$

Taking Boolean disk sensing model for example:

$$p(x) = \begin{cases} 1, & x \leq R, \\ 0, & x > R, \end{cases} \quad (2)$$

Therefore, under Boolean disk model,  $\lambda_c = \pi R^2 d$ . Given an arbitrary sensing model, the value of  $\lambda_c$  can be analogically calculated following equation (1).

Each sensor node is assumed to have a scheduling period of  $T$  and working time  $T_w$ ,  $0 < T_w \leq T$ ; thus  $\beta = T_w / T$  is the duty cycle ratio. Each node can choose its wake-up point  $t_s$  within  $[0, T)$  and wakes up for a period of time  $T_w$ , and then goes back to sleep until  $T + t_s$ . We assume all the events are stationary and persistent, e.g., a localized fire. It is required that the events be detected within a delay bound  $\tau$ .

### 3.2. Detection Analysis

*Proposition 1:* Suppose duty-cycled sensor nodes are deployed conforming to homogeneous P.P.P. in an area  $A$  and the event arrival follows uniform distribution, the probability that any event be captured within delay bound  $\tau$  is:

$$P_s(t < \tau) = \frac{1 - e^{-\lambda_c(\frac{\tau}{T} + \beta)}}{1 - e^{-\lambda_A}}, \quad 0 < \beta \leq 1 - \frac{\tau}{T}, \quad (3)$$

*Proof:* First, the probability that there are  $k$  nodes in the area  $A$  is  $\frac{\lambda_A^k}{k!} e^{-\lambda_A}$ ,  $k = 0, 1, 2, \dots$ . The

probability that no nodes are in the area ( $k = 0$ ) is  $e^{-\lambda_A}$ . Therefore, the probability that there is at least one node in the area is  $1 - e^{-\lambda_A}$ . Second, if the probability of an event occurring in a sensor's coverage area is  $g$ , and since the average number of nodes within the coverage area of a sensor is  $\lambda_c$ , the probability of an event being captured at least by one sensor is:

$$P_o = 1 - e^{-g\lambda_c}, \quad (4)$$

Now we consider an arbitrary point of interest to be monitored. Suppose node  $S$  is the only node covering the point. The duty cycle of node  $S$  is stated in Section 3.1. Since the sensor has a probability  $\beta$  of being awake, we have  $P_o(t = 0) = \beta$ . The probability density function (PDF) of the detection delay  $t$  is  $f(\tau)$ , where  $0 < \tau \leq T - \beta T$ , which conforms to a uniform distribution, thus  $f(\tau) = \frac{1}{T}$ , as long as the event occurs uniformly anywhere within the duty cycle. Therefore, when there is only one sensor covering the point, the cumulative probability distribution for the detection delay is:

$$P_o(t < \tau) = \beta + \frac{\tau}{T}, \quad 0 < \tau \leq T - \beta T, \quad (5)$$

When there are  $k$  nodes covering the point, we substitute the  $g$  in equation (4) with equation (5) and get the probability that an event is captured within an interval time no larger than  $\tau$ :

$$P_o = 1 - e^{-\lambda_c(\frac{\tau}{T} + \beta)}, \quad (6)$$

Since we focus on those points that are in the area, the cumulative density function (CDF) of the detection delay for such points is

$$P_s(t < \tau) = \frac{1 - e^{-\lambda_c(\frac{\tau}{T} + \beta)}}{1 - e^{-\lambda_A}}, \quad \text{where } \lambda_c \text{ is given in equation (1).}$$

### 3.3. Discussions

We now discuss the implications of our analytical results. When the delay bound  $\tau = 0$ , it means the event should be instantly detected. With the increase of  $\tau$ , the real-time detection probability becomes larger on average. This is because more events can be captured with relaxed detection deadline. In order to save energy, the duty cycle factor  $\beta$  should not be set large. If it is larger than  $1 - \frac{\tau}{T}$ , the delay bound  $\tau$  will lose all meaning. With the increase of node density, both  $\lambda_A$  and  $\lambda_c$  become larger. The real-time detection probability approaches 1 when the node

density is sufficiently large, independent of the duty cycle  $\beta$ .

## 4. Numerical Simulations

In this section, numerical simulations are conducted under various sensing models to check whether simulation results match analytical predictions. The regular sensing models adopted include Boolean disk model, power-law model, exponential model and staircase model. For Boolean disk model,  $p(x)$  is given in equation (2). For power-law model, exponential model and staircase model, the expressions of  $p(x)$  are respectively given in equations (7), (8) and (9), and their examples are demonstrated in Fig. 1(a).

$$p(x) = \begin{cases} 1, & x \leq r_s, \\ \frac{\alpha}{x^\eta}, & r_s < x \leq r_u, \\ 0, & x > r_u. \end{cases}, \quad (7)$$

$$p(x) = \begin{cases} 1, & x \leq r_s, \\ e^{-\omega(x-r_s)^\beta}, & r_s < x \leq r_u, \\ 0, & x > r_u. \end{cases}, \quad (8)$$

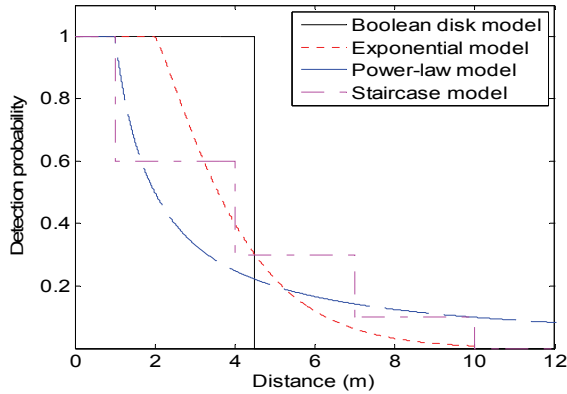
$$p(x) = \begin{cases} 1, & x \leq r_s, \\ p_1, & r_s < x \leq l_1, \\ p_2, & l_1 < x \leq l_2, \\ p_3, & l_2 < x \leq r_u, \\ 0, & x > r_u. \end{cases}, \quad (9)$$

With the expressions of  $p(x)$ , respective  $\lambda_c$  for each sensing model can be calculated by equation (1).

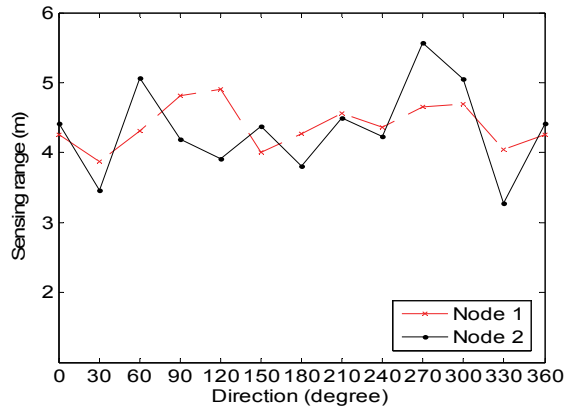
Experimental tests show that the realistic sensing range is anisotropic. Therefore we also incorporate the anisotropic sensing model into simulations to test the robustness of the performance predictions. It is concluded from the experimental data set of ExScal Mote [7] that the sensing range in one direction can be approximated by a normal distribution  $N(217, 32^2)$ (inches). We scaled the normal distribution  $N(217, 32^2)$ (inches) to  $N(4.5, 0.7^2)$ (m) to fit the simulation settings. For simplicity, we use linear interpolation to specify the boundary of the sensing area. As an example, the approximation of the two representative nodes based on this model are shown in Fig. 1(b), which accurately reflects the fluctuations of sensing ranges in different directions. We use the same formulas as the previous idealistic experiments.

In the simulations, locations of nodes are generated over an area of the size  $50\text{m} \times 50\text{m}$ , conforming to a homogeneous P.P.P. The period  $T$  is

chosen to be 1 s. The waking points of the nodes are generated according to a uniform distribution over [0 s, 1 s). The parameters for different sensing models are listed in Table 1.



(a) Regular sensing models.



(b) Anisotropic sensing models.

Fig. 1. Illustration of different sensing models.

Table 1. Parameter settings for different sensing models.

| Sensing Models     | Parameter Settings   |
|--------------------|--|
| Boolean disk model | $R = 4.5$ m  |
| Power-law model    | $r_s = 1$ m, $r_u = 14$ m, $\alpha = 1$ ,<br>$\eta = 1$  |
| Exponential model  | $r_s = 2$ m, $r_u = 10$ m,<br>$\omega = 0.4$ , $\beta = 1.2$                                       |
| Stair-case model   | $r_s = 1$ m, $l_1 = 4$ m,<br>$l_2 = 7$ m, $r_u = 10$ m,<br>$p_1 = 0.6$ , $p_2 = 0.3$ , $p_3 = 0.1$ |
| Anisotropic model  | $R \sim N(4.5, 0.72)$ m  |

We choose 200 random points each time to be the target locations and run the simulation. The simulation repeats 50 times and we calculate the average values. In the first set of simulations, the parameter  $\lambda_A$  is set to 250 with node density  $d = 0.1$ . We record the average detection probability given the detection delay bounds equal to 0s, 0.1s, ..., 0.9 s, and 1 s. Various  $\beta$  values are also considered (0.1, 0.2, 0.3 and 0.4). We then compare these simulated

detection probabilities with the analytical results obtained by equation (3). The comparison results are shown in Fig. 2 (a)–(e), under respective sensing models. From Fig. 2 we can see that the simulation results conform to the analytical ones very well, which validate our proposition in Section 3.2.

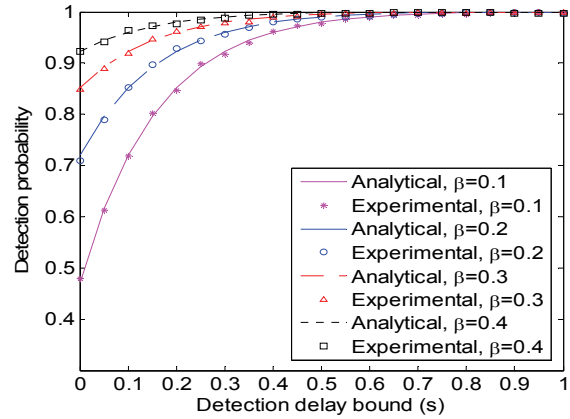


Fig. 2 (a). Detection probability vs. delay bound with different duty cycles, node density  $d = 0.1$  – Boolean disk model.

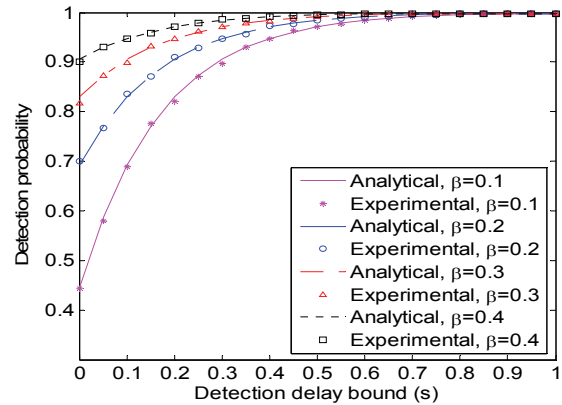


Fig. 2 (b). Detection probability vs. delay bound with different duty cycles, node density  $d = 0.1$  – Exponential model.

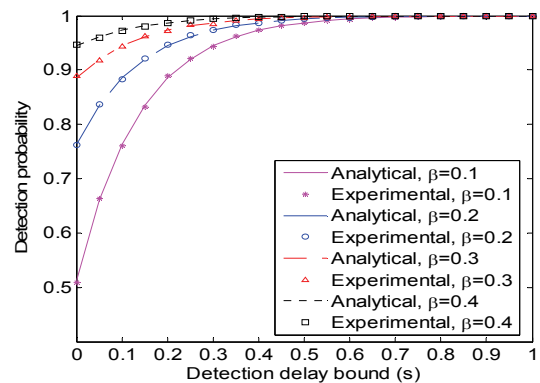
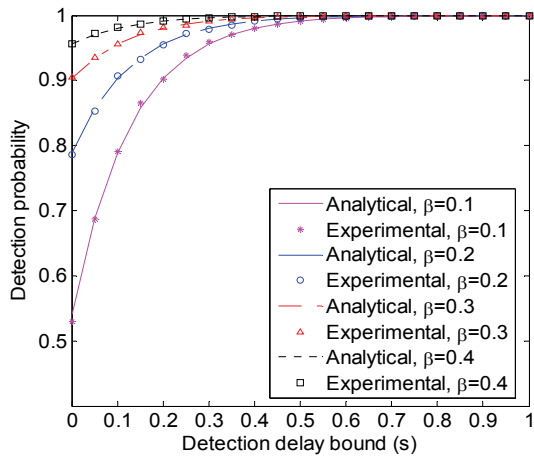
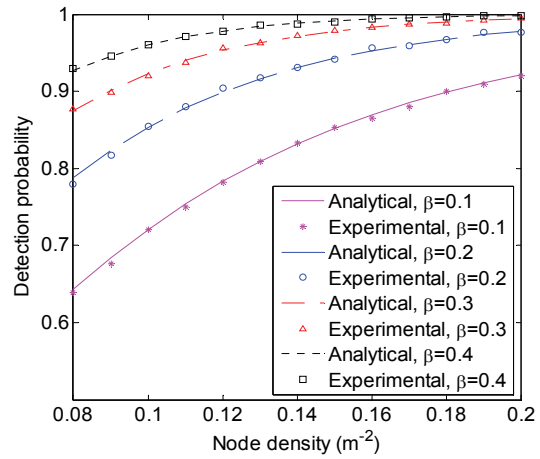


Fig. 2 (c). Detection probability vs. delay bound with different duty cycles, node density  $d = 0.1$  – Power-law model.



**Fig. 2 (d).** Detection probability vs. delay bound with different duty cycles, node density  $d = 0.1$  – Staircase model.



**Fig. 3 (a).** Detection probability vs. node density with different duty cycles, delay bound  $\tau = 0.1$  – Boolean disk model.

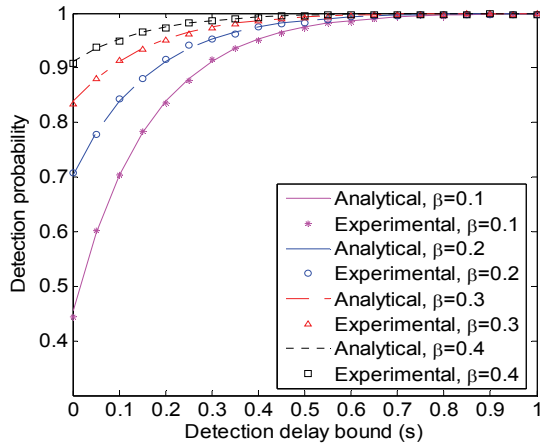


**Fig. 2 (e).** Detection probability vs. delay bound with different duty cycles, node density  $d = 0.1$  – (c) Anisotropic model.

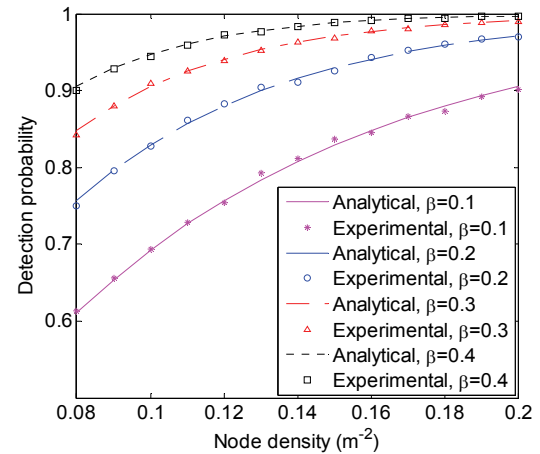


**Fig. 3 (b).** Detection probability vs. node density with different duty cycles, delay bound  $\tau = 0.1$  – Exponential model.

In the second set of simulations, we choose various node density values (0.08, 0.1, ..., 0.2) and  $\beta$  values (0.1, 0.2, 0.3 and 0.4), and run the simulations to gather the average detection probabilities. Other settings are the same as the previous set of simulations. We compare the average detection probabilities with the analytical probabilities obtained by equation (3) and plot Fig. 3. The figures show that under arbitrative sensing models, the average detection probabilities obtained by simulations are very close to the analytical results.

Regarding these results we have two major observations. First, sensing irregularity has a very small effect on the final results. One reason is that even though the sensing ranges vary with different directions, the overall degree of coverage for the area remains almost the same, approximated by  $\lambda_c$ . Therefore, the overall detection delay distribution is almost not affected. Second, the maximal error relative to analytical predictions is no more than 2.4 %.

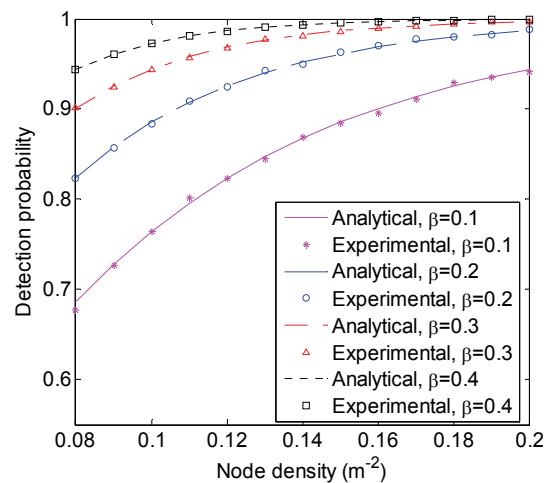


**Fig. 3 (c).** Detection probability vs. node density with different duty cycles, delay bound  $\tau = 0.1$  – Power-law model.

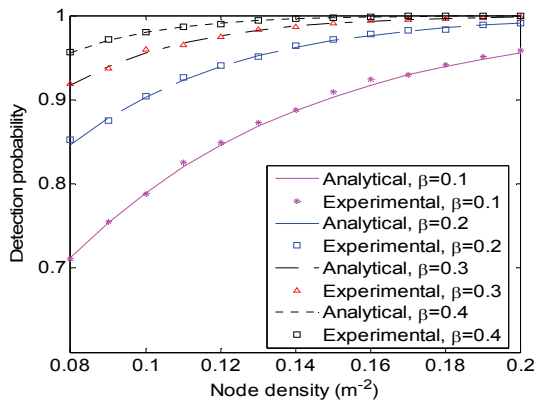


**Fig. 3(d).** Detection probability vs. node density with different duty cycles, delay bound  $\tau = 0.1$  – Staircase model.

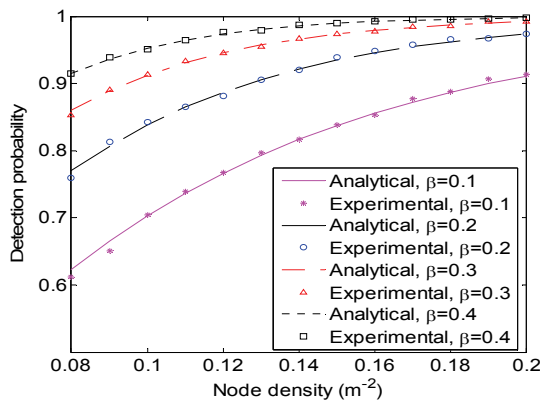


**Fig. 3(e).** Detection probability vs. node density with different duty cycles, delay bound  $\tau = 0.1$  – Anisotropic model.

That is, suppose we have a set of system parameters that guarantee 99 % successful detection within the delay bound. Then, the actual detection rate should be no less than 96 %. Based on the above observation, we conclude that our model is quite robust to most sensing conditions. However, there are still types of sensors which may exhibit different characteristics and may have varied effect on the detection performance. However, we envision that with a relatively large system with considerable density, the effect of sensing irregularity will be considerably limited.

## 5. Conclusions

In this paper, closed-form expressions are derived for distribution of real-time detection delay. Various sensing models are adopted in the numerical

simulations to validate the analytical closed-form results. It is shown that under all these sensing models adopted, the numerical results always closely matches the analytical ones. The analytical results are highly important for understanding the relationship between the surveillance quality and system parameters under different real-time requirements and arbitrary sensing models. Designers can apply these analytical results to predict the detection performance without costly deployment and testing. They can make decisions on key system or protocol parameters, such as the network density and the duty cycle, according to the detection requirements of the system.

## Acknowledgements

The authors acknowledge the support from the National Natural Science Foundation of China (No.61003264) and Zhejiang Provincial Natural Science Foundation of China (No. LY13F020028).

## References

- [1]. S. Pattem, S. Poduri, and B. Krishnamachari, Energy-quality tradeoffs for target tracking in wireless sensor networks, in *Proceedings of the 2<sup>nd</sup> International Conference on Information Processing in Sensor Networks*, Palo Alto, California, USA, April 22-23, 2003, pp. 32-46.
- [2]. Q. Cao, T. Yan, J. Stankovic, and T. Abdelzaher, Analysis of target detection performance for wireless sensor networks, *Lecture Notes in Computer Science*, Vol. 3560, 2005, pp. 276-292.
- [3]. T. He, P. Vicaire, T. Yan, L. Luo, L. Gu, G. Zhou, R. Stoleru, Q. Cao, J. A. Stankovic, and T. Abdelzaher, Achieving real-time target tracking using wireless sensor networks, in *Proceedings of the 12<sup>th</sup> IEEE Real-Time and Embedded Technology and Applications Symposium*, April 4-7, San Jose, California, USA, pp. 37-48.
- [4]. P. Vicaire, T. He, Q. Cao, T. Yan, G. Zhou, L. Gu, L. Luo, R. Stoleru, J. A. Stankovic, and T. F. Abdelzaher, Achieving long-term surveillance in VigilNet, *ACM Transactions on Sensor Networks*, Vol. 5, 2009, pp. 1-39.
- [5]. S. Zahedi, M. Srivastava, L. Kaplan, and C. Bisdikian, Quality tradeoffs in object tracking with duty-cycled sensor networks, in *Proceedings of the 31<sup>st</sup> IEEE Real-Time Systems Symposium*, San Diego, CA, November 29-December 2, 2010, pp. 160-169.
- [6]. Y. Zhu, Y. Liu, and L. M. Ni, Optimizing event detection in low duty-cycled sensor networks, *Wireless Networks*, Vol. 18, Issue 3, 2012, pp. 241-255.
- [7]. ExScale mote. (<http://www.cast.cse.ohio-state.edu/exscal/>)